

Solutions, With and Without Chemical Reaction," *Chem. Eng. Sci.*, **10**, 88-104 (1959).
Nysing, R. A. T. O. and H. Kramers, "Absorption of CO₂ in Carbonate Bicarbonate Buffer Solutions in a Wetted Wall Column," *ibid.*, **8**, 81-89 (1958).
Ruschak, K. J., and L. E. Scriven, "Developing Flow on a Vertical Wall," *J. Fluid Mech.*, **81**, 305-306 (1977).

Wilkes, J. O., and R. M. Nedderman, "The Measurement of Velocities in Thin Films of Liquid," *Chem. Eng. Sci.*, **17**, 177-187 (1962).

Manuscript received June 16, 1977; revision received February 13, and accepted March 6, 1978.

Liquid-Solid Mass Transfer in Packed Beds with Downward Concurrent Gas-Liquid Flow

CHARLES N. SATTERFIELD

MICHAEL W. VAN EEK

and

GARY S. BLISS

Department of Chemical Engineering
Massachusetts Institute of Technology
Cambridge, Massachusetts 02139

Mass transfer coefficients were determined by measuring the rate of solution of cylindrical 3 or 6 mm benzoic acid tablets into water in the presence of flowing nitrogen, helium, or argon. Gas flow rates varied from 0 to 1.6 kg/(m²·s) and liquid flow rates from 0.5 to 25 kg/(m²·s), resulting in hydrodynamic flow patterns varying from trickle to turbulent pulse types of flow. In the pulse regime, the mass transfer coefficient was markedly affected by gas flow rate but did not depend on gas density explicitly if correlated in terms of an energy dissipation function.

SCOPE

It is necessary to be able to characterize liquid-solid mass transfer in packings representative in size and shape to those encountered in industrial trickle-bed reactors and at gas and liquid flow rates representative of industrial practice in order to understand some of the reasons for the performance of existing reactors and to design and scale-up new reactors.

Until fairly recently, the only information available was a study by van Krevelen and Krekels (1948) in the absence of forced gas flow. During the course of the present work, several other studies were published (Table I) based in almost all cases on measurements of the rate of solution of a slightly soluble organic material in water in the pres-

ence of air or nitrogen. In the present work, mass transfer coefficients were similarly determined by measuring the rate of solution into distilled water of benzoic acid cylindrical tablets, 3 × 3 or 6 × 6 mm in size. However, a wide range of flow conditions was covered, from single phase liquid flow in the presence of stagnant gas to highly pulsing gas-liquid flow. Liquid flow rates were varied from 0.5 to 25 kg/(m²·s). Gas flow rates were varied from 0 to 1.6 kg/(m²·s) and encompassed a tenfold variation in gas density by use of helium and argon as well as nitrogen. The mass flow rates of liquid and gas studied encompass essentially the whole range of interest in industrial trickle-bed reactors.

CONCLUSIONS AND SIGNIFICANCE

The nature of the flow regime has a major influence on the rate of mass transfer, and different types of correlations are applicable in different regimes.

Results were obtained in terms of the product $k_S\phi$, where k_S is the liquid-solid mass transfer coefficient, and ϕ , which was not measured separately, is the fraction of the external surface area of the packing that is wetted with flowing liquid. Values of $k_S\phi$ varied by a factor of about 50 over the range of conditions studied and are expressed in terms of a Sherwood number. At a constant gas flow rate and particle size, $k_S\phi$ always increased with increased liquid flow rate. At fixed liquid flow rate and particle size, increasing gas flow rate from zero increased mass transfer by a maximum of only about 10% within the trickle regime but increase to cause pulsing increased mass transfer by a factor of as much as 2.6. A decrease in particle diameter from 6×10^{-3} to 3×10^{-3} m caused an increase in $k_S\phi$ in all flow regimes.

A packed bed may be caused to flood deliberately, for example, by forcing the liquid exiting from the bed to flow upwards through an external tube before allowing it to flow downwards again. At zero or low gas flow rate, when the bed is not caused deliberately to flood, the true hydrodynamic flow pattern may be trickle flow with incomplete or complete wetting, or the bed may instead flood naturally, as shown schematically on Figure 8.

Correlations are presented for predicting mass transfer in the various regimes, and present results are compared and contrasted to previous studies. For incomplete wetting ($Re < 60$), our data and the data of Specchia et al. (1976) for cylinders are correlated by Equation (4). For flooded flow, mass transfer is well predicted by the equation of Carberry (1960) rewritten for cylinders as Equation (3). In the pulse regime, mass transfer coefficients are well described by an energy dissipation function, Equation (13). When thus expressed, the mass transfer coefficient did not depend explicitly on gas density.

0001-1541-78-9476-0709-\$01.05. © The American Institute of Chemical Engineers, 1978.

TABLE 1. SUMMARY OF PREVIOUS RELEVANT STUDIES

Author	Packing shape	Packing material	d_p or $d_p \times 1_p$ ($10^{-3}m$)	Type of gas	Type of liquid	G , $kg/(m^2 \cdot s)$	L , $kg/(m^2 \cdot s)$
van Krevelen and Kerkels (1948)	Granular	Benzoic acid	2.9 to 1.4	—	Water, aq. glycerol	0	0.12 to 3.7
Sato et al. (1972)	Granular Spheres	Sulfur Benzoic acid	9-12 5.5, 12.2	— Nitrogen(?)	Benzene Water	0.011 to 1.19 (as N_2)	10 to 200
Lemay et al. (1975)	Spheres	Benzoic acid + rhodamine B	6.25	Air	Water	0.37 to 0.90	13 to 40
Goto and Smith (1975a)	Granular	β -naphthol	2.4, 0.54	Air	Water	0 to 0.009	0.48 to 5.2
Goto et al. (1975)	Granular	β -naphthol	2.4	Air	Water	0 to 0.009	0.48 to 5.2
Sylvester and Pitayagulsarn (1975)	Granular Cylinders	Naphthalene Benzoic acid	0.54, 1.08, 2.4 3.17 \times 3.17	Air	Water	0 to 0.009 0.23 to 0.93	0.48 to 5.2 3.5 to 19.7
Specchia et al. (1976)	Cylinders	Benzoic acid	3 6	Air	Water	0 to 1.9	1.6 to 8.3
				Air	Water, water + surfactants, water + glycerol		
Hirose et al. (1976)	Spheres	Benzoic acid Brass	2.8, 5.5, 12 3.2, 6.4, 12.7	Nitrogen(?) Nitrogen(?)	Water Potassium dichromate in aqueous sulfuric acid	0 to 2.3	0.53 to 245

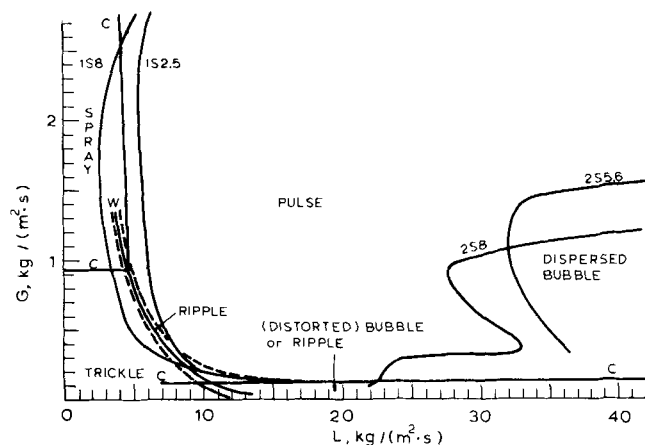


Fig. 1. Flow regimes: C = Charpentier et al. (1971) 3 mm spheres, 1S = Sato et al. (1972) 8 or 2.5 mm spheres, 2S = Sato et al. (1973) 8 or 5.6 mm spheres, W = Weekman and Myers (1964) 3.8 to 6.5 mm spheres.

Mass transfer between a flowing liquid and a bed of solid particles in the presence of a flowing gas is of concern in a variety of chemical engineering applications. Of immediate interest here was the nature of this process in a reactor in which a liquid and a gas pass concurrently downward through a packed bed of catalyst particles. For succinctness, the term trickle bed is frequently used to refer to any system of this type, although in fact the hydrodynamic behavior varies considerably with conditions, as will be described.

The objective of this study was to characterize liquid-solid mass transfer in packings representative of industrial catalysts and at gas and liquid flow rates typically encountered in industrial reactors. A recent review (Satterfield, 1975) describes trickle-bed reactors in general and other aspects of their mass transfer characteristics.

At the onset of this work, only one paper had appeared in the literature on the subject, a study by van Krevelen and Kerkels (1948) in the absence of forced gas flow. During the course of our investigation, at least seven other closely related studies were published, which are compared and contrasted to our results.

FLOW REGIMES

An understanding of the nature of the flow regime and how it changes with operating variables is important in interpreting and correlating mass transfer effects. Figure 1 summarizes a number of studies by showing the boundaries between different flow regimes as reported by various investigators for nonfoaming air-water systems. Actually, of course, the transition between regimes is gradual, and the boundaries are also affected by particle size and shape. They would also be altered by the physical properties of other liquids and gases and by the particular point in the bed at which observations are made, since the flow pattern can change with axial position. Table 1 summarizes some of the more important experimental variables in previous relevant mass transfer studies, and Figure 1 helps provide orientation as to the type of flow pattern that was probably encountered in each.

The region of primary industrial interest encompasses liquid mass flow rates of about 0.5 to 25 $kg/(m^2 \cdot s)$, equivalent to superficial velocities of 6 to 290 ft/hr for a liquid of unit specific gravity. In hydrotreating of fuels, as in hydrotreating, hydrodesulfurization, hydrocracking, etc., gas to liquid ratios range from about 500 to 10 000 SCF of hydrogen/bbl of liquid. Gas mass flow

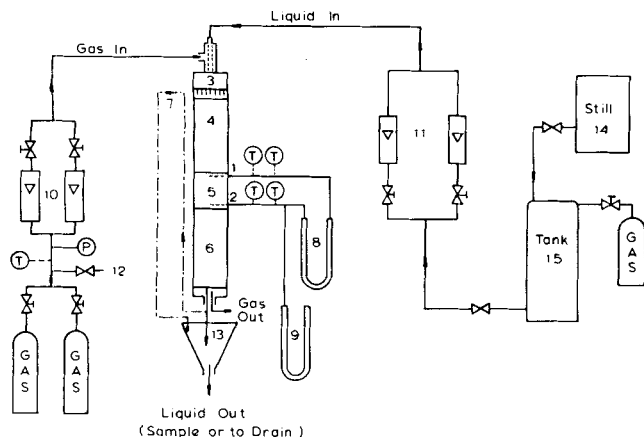


Fig. 2. Apparatus.

rates up to about $1.6 \text{ kg}/(\text{m}^2 \cdot \text{s})$ are a reasonable reflection of these industrial conditions.

The flow regimes of particular interest here are those described as trickle, ripple, and pulse. Generally speaking, these are encountered successively as one increases liquid flow rate at a constant gas rate, or vice versa. In the trickle regime, the liquid flows over the packing under the effect of gravity in essentially laminar films or rivulets which, however, may not be in contact with one another. The pressure drop as recorded by a manometer does not fluctuate. As gas or liquid flow rate is increased, the liquid appears to become more turbulent, and many small ripples are seen. Occasional pulses may appear near the bottom of the column. The pulse regime is characterized by a large degree of turbulence in the bed, with a visible pulsing of sections of higher density (mostly liquid) and lower density (mostly gas) through the column. The pulse regime first developed at the exit and, with fixed liquid rate, occurred further towards the top of the column as gas flow was increased.

EXPERIMENTAL APPARATUS AND PROCEDURE

Liquid-solid mass transfer was determined by measuring the rate of dissolution of a sparingly soluble solute, benzoic acid, in distilled water in the presence or absence of nitrogen or another gas, with the apparatus shown in Figure 2. The trickle bed was a circular glass column approximately 70 cm long and with an inside diameter of 6.96 cm, packed in three sections. The dissolving section in the center (5) contained benzoic acid cylindrical tablets, which had been made in a tabletting press, either approximately 6×6 or 3×3 mm. The inert entrance section (4) and the inert exit section (6) contained cylindrical particles of nearly the same size as the benzoic acid tablets, made of aluminum oxide or aluminum oxide/silicon oxide. The pellets in the inert exit section were nonporous and rested on a 16×16 mesh stainless steel screen.

Pressure drop and temperature were measured at the pressure taps (1 and 2) by manometers (8 and 9) and thermocouples, respectively. Various manometer fluids were used, depending on the pressure drop. Manometer 9 measured the pressure drop between point 2 and the atmosphere.

Prepurified gas and the distilled water were introduced at the top of the column through a distributor (3) which had been carefully designed so as to provide excellent uniform initial distribution of gas and liquid. The outlet plate of the distributor had forty-three liquid outlets and eighteen gas outlets. The gas supply was obtained from two cylinders connected in parallel, and the gas flow rate was measured by one of the two rotameters (10), depending on the flow rate. Distilled water was produced in a still (14) and then stored in an approximately 250 l stainless steel tank (15). Purified nitrogen from a cylinder was used to pressurize the tank to 20 or 30 lb/in.² gauge. The liquid flow rate was metered by

one of the two rotameters (11), depending on the flow rate. After passing through the bed, the gas was vented to the atmosphere and the liquid flowed into a funnel (13), either directly or via a bed flooder and bed flooder draining tube (7). From the funnel the liquid flowed into the exit line from which timed samples of liquid could be taken when desired.

It was considered desirable to compare results obtained in trickle flow at zero gas rate with results obtained in flooded flow at the same superficial liquid velocity. In the trickle regime, liquid falls onto the packing at the top of the column and trickles through the packing under the effect of gravity. In flooded flow, liquid flows through the packing by forced convection, and liquid fills all the void space between particles. Generally, the column was first operated in the flooded state and then after being drained, in the trickle regime at the same superficial liquid flow rate and zero gas rate, before (still at the same liquid flow rate) proceeding to a finite gas rate. Here measurements were made at each of one or several gas flow rates, the superficial liquid rate being kept constant. (At no time during the draining of the bed from the flooded state was the liquid flow into the column decreased or stopped.) The bed was caused to flood by forcing the exiting liquid to flow upwards through an external tube (the bed flooder) before allowing it to flow downwards again (through the bed flooder draining tube).

Upon introducing new flow conditions, for example, going from flooded flow to the trickle regime at zero gas flow rate, a transition period was encountered of considerable length, especially at a low liquid flow rate, before a new steady state rate of mass transfer was observed. These times were usually much longer than would be calculated for flush out of liquid from the exit inert packing section, even if we assume that this section behaved as a CSTR, and it appears that considerable time (compared to that for flush out of the liquid) was required under some conditions for a new steady state degree of wetting to be reached after the flow pattern was changed by changing the gas flow rate.

The ratio of dissolving section height to tablet diameter was at least 16, and the percent saturation of exit liquid was at most 65% (which was only for flooded flow) and usually between 9 and 40%. Mass transfer coefficients were calculated by Equation (1), which assumes plug flow of the liquid.

$$k_s \phi = \frac{L_v A_c}{A_p} \ln \left[\frac{1}{1 - (c_{\text{exit}}/c_{\text{sat}})} \right] \quad (1)$$

The value of c_{exit} was determined by titration with sodium hydroxide. The length of any run was limited so that the change in A_p from beginning to end as the packing dissolved typically did not exceed about 11%. The pellets remained smooth during solution, and calculations assumed that the cylindrical shape was maintained but allowance was made for the decrease in A_p . The fractional wetting of the particles was not measured directly, so the results yield values of the product $k_s \phi$.

The heights of the dissolving section, the inert entrance section, and the inert exit section were typically 10.7, 20.9, and 21.8 cm, respectively, for the 6 mm cylinders and 5.8, 17.9, and 29.3 cm, respectively, for the 3 mm cylinders.

Bliss (1976) studied the dissolution of 3 mm benzoic acid cylindrical tablets into water in the presence of helium, nitrogen, or argon in order to determine some effects of gas density. The liquid flow rate was kept fixed at $5 \text{ kg}/(\text{m}^2 \cdot \text{s})$, and the gas flow rate was varied over a wide range such that trickle type of flow was observed at the lower rates and pulse type of flow at the higher rates.

REPRESENTATIVE RESULTS AND DISCUSSION

Experiments were conducted at about room temperature at liquid Schmidt numbers between 940 and 2114 and liquid Reynolds numbers between 1.50 and 196. Reynolds and Sherwood numbers were based on d_p' , the equivalent particle diameter.

Results are presented in terms of $Sh \phi / Sc^{1/3}$ rather than $k_s \phi$, since there were small variations in temperature between different runs. Convective mass transfer at a

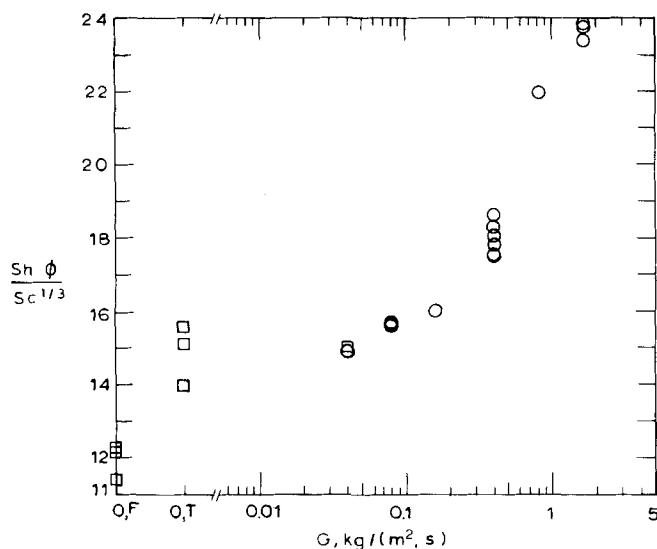


Fig. 3. Effect of gas flow rate on $Sh\phi/Sc^{1/3}$, $L = 4.9 \text{ kg}/(\text{m}^2 \cdot \text{s})$ and $d_p = 6 \times 10^{-3} \text{ m}$. Ripple regime and incipient pulsing at $G = 0.4$.

high Schmidt number would be expected to be correlated by this ratio, with a one third power on Sc . The liquid viscosity varied between extremes of 0.90×10^{-3} and $1.23 \times 10^{-3} \text{ kg}/(\text{m} \cdot \text{s})$. The liquid density was taken to be constant at $1000 \text{ kg}/\text{m}^3$.

A meaningful correlation of data can proceed only from recognition of certain phenomena which significantly affect the results. The two most important here are:

1. The hydrodynamic flow pattern.
2. The partial and erratic wetting of packing and the effect on this of preflooding. Various reports in the literature and our own inspection indicate that wetting cannot be assumed to be complete at liquid flow rates below about 5 to $10 \text{ kg}/(\text{m}^2 \cdot \text{s})$.

Both phenomena are affected by the gas and liquid flow rates and particle size. Figures 3 through 6 show some typical results for representative combinations of L , G , and d_p and some measure of the degree of scatter of the data. In these figures, circles and triangles at any one value of G indicate data taken at different times from the start of a run, holding G constant, but after a steady state value of $Sh\phi/Sc^{1/3}$ had been reached. A square indicates the average of a steady state time series during any one run, and several squares indicate the results of several steady state time series. The spread between circles in the trickle and ripple regimes is probably caused in part by erratic wetting of the solid about some steady state average value of ϕ . The spread between squares is an indication of reproducibility of results. The symbol O, F on the abscissa refers to single-phase flooded condition and O, T to trickle flow conditions at zero gas velocity. All results shown in Figure 3 through 6 were obtained with nitrogen as the gas phase.

$L = 4.9 \text{ kg}/(\text{m}^2 \cdot \text{s})$; $d_p = 6 \times 10^{-3} \text{ m}$ (Figure 3)

The average value of $Sh\phi/Sc^{1/3}$ for flooded flow at zero gas rate was $11.9 \pm 4.5\%$. Changing to the trickle regime ($G = O, T$) increased this value by about 25%, even though ϕ decreased from unity. This trend agrees with findings reported by Goto and Smith (1975a), Goto et al. (1975), and Hirose et al. (1976) and can be attributed to an increase in interstitial liquid velocity caused by the decrease in liquid holdup from ϵ . The average value was $14.9 \pm 6.2\%$. One would expect the reproducibility to be less in the trickle regime than for flooded flow as the added complication of incomplete (and erratic) wetting appears.

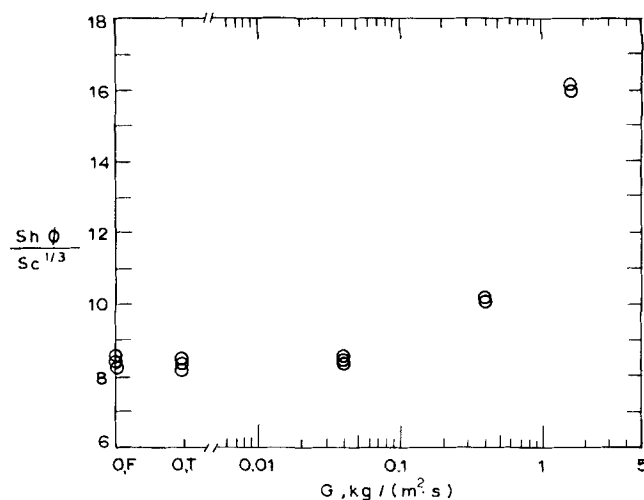


Fig. 4. Effect of gas flow rate on $Sh\phi/Sc^{1/3}$, $L = 4.9 \text{ kg}/(\text{m}^2 \cdot \text{s})$ and $d_p = 3 \times 10^{-3} \text{ m}$. Pulse regime had been entered at $G = 0.4$.

Introducing a low gas flow caused no significant change in the mass transfer rate. At a gas flow rate of $0.40 \text{ kg}/(\text{m}^2 \cdot \text{s})$, a significant interaction between gas and liquid started taking place with rippling, incipient pulsing and accompanying turbulence, and the mass transfer began to increase significantly. At $G = 0.80$, the bed was operating in the very turbulent pulse regime, and at $G = 1.64$, $Sh\phi/Sc^{1/3}$ was 59% higher than at $G = O, T$.

A gas flow can increase liquid-solid mass transfer in a trickle-bed system in three ways: by increasing the wetting factor ϕ , by decreasing the liquid holdup and therefore increasing the interstitial liquid velocity, and by introducing or increasing the level of turbulence in the system. All of these mechanisms are important and are noticed especially as the system enters the pulse regime. The significant increase in mass transfer upon entering the pulse regime was also noticed by Hirose et al. (1976).

$L = 4.9 \text{ kg}/(\text{m}^2 \cdot \text{s})$; $d_p = 3 \times 10^{-3} \text{ m}$ (Figure 4)

Comparison of Figure 4 with Figure 3 shows the effect of a smaller particle size. Here, the values of $Sh\phi/Sc^{1/3}$ for flooded flow and in the trickle regime at zero gas rate are just about equal, whereas with 6 mm particles, mass transfer in the trickle regime was higher than in flooded flow. It appears that the decrease in mass transfer caused by decreased wetting in the trickle regime (from that in flooded flow) counterbalanced the increase in mass transfer caused by the decrease in liquid holdup and increase in interstitial liquid velocity upon going from flooded to trickle conditions. Again, a low gas flow rate did not cause any increase in mass transfer. At $G = 0.4 \text{ kg}/(\text{m}^2 \cdot \text{s})$, the pulse regime had been entered and the mass transfer increased by 22%. At $G = 1.65 \text{ kg}/(\text{m}^2 \cdot \text{s})$, the mass transfer was 94% greater than at $G = O, T$.

The effect of decreasing particle diameter was to increase $k_s\phi$, both in flooded flow and in the trickle regime, since $Sh\phi/Sc^{1/3}$ contains d_p as a variable but does not double between 3 and 6 mm cylinders. Results by Gianetto (1976) show that at zero gas rate in the trickle regime and at this liquid flow rate, ϕ is about 10 to 15% lower for 3 mm cylinders than for 6 mm ones. Taken together with the results for $Sh\phi/Sc^{1/3}$, this means that at zero flow rate k_s itself (without ϕ) in both flooded flow and the trickle regime is higher for 3 mm cylinders than for 6 mm cylinders.

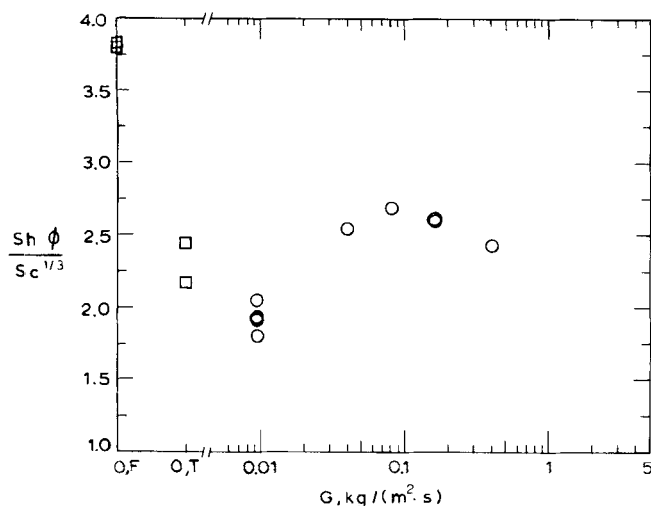


Fig. 5. Effect of gas flow rate on $Sh\phi/Sc^{1/3}$, $L = 0.48 \text{ kg}/(\text{m}^2 \cdot \text{s})$ and $d_p = 6 \times 10^{-3} \text{ m}$. No pulse regime.

$L = 0.48 \text{ kg}/(\text{m}^2 \cdot \text{s})$; $d_p = 6 \times 10^{-3} \text{ m}$ (Figure 5)

Figure 5, in contrast to Figure 3, shows that at a low liquid flow rate, mass transfer is much less, as would be expected. Going from flooded flow to the trickle regime produced a marked drop in $Sh\phi/Sc^{1/3}$. Presumably, the wetting factor ϕ in the trickle regime at $G = 0, T$ was low enough (probably smaller than 0.5) to outweigh the increased interstitial velocity effect.

Overall, the effect of gas flow rate at this low liquid flow rate, where no pulse regime is encountered, seems to be small and erratic. This agrees with the findings of Hirose et al. (1976).

$L = 25 \text{ kg}/(\text{m}^2 \cdot \text{s})$; $d_p = 6 \times 10^{-3} \text{ m}$ or $3 \times 10^{-3} \text{ m}$ (Figure 6)

Comparison of Figure 6 with Figures 3 and 4 reveals the considerable effect of increased liquid velocity on mass transfer at any specified gas velocity, for either size of packing.

As was the case at $L = 4.9$, mass transfer here increased upon going from flooded flow to the trickle regime for the 6 mm particles. However, with the 3 mm particles, the bed flooded itself, and a true trickle regime did not develop. In general, at sufficiently high liquid flow rates and/or sufficiently small particle diameters, a trickle regime will not exist at $G = 0$, and the bed floods naturally.

The effect of introducing a gas flow at $L = 25 \text{ kg}/(\text{m}^2 \cdot \text{s})$ was marked. The liquid holdup, which at $G = 0$ was originally close or equal to the void fraction ϵ , decreased considerably. A great amount of turbulence was also created in the bed as the regime changed from trickle to pulse.

The effect of decreasing particle diameter at $L = 25$ (where $\phi = 1$ at $G = 0, T$ for both particle sizes) was again to increase k_s , both at $G = 0, F$ and $G = 0, T$.

Further Observations

The largest mass transfer coefficient $k_s\phi$ measured was $1.21 \times 10^{-4} \text{ m/s}$ at $L = 25 \text{ kg}/(\text{m}^2 \cdot \text{s})$, $G = 1.63 \text{ kg}/(\text{m}^2 \cdot \text{s})$, and d_p about $3 \times 10^{-3} \text{ m}$. The smallest mass transfer coefficient $k_s\phi$ measured was $2.27 \times 10^{-6} \text{ m/s}$ at $L = 0.48 \text{ kg}/(\text{m}^2 \cdot \text{s})$, $G = 0.0094 \text{ kg}/(\text{m}^2 \cdot \text{s})$, and a d_p of about $6 \times 10^{-3} \text{ m}$, constituting a range of variation of about 50.

The effect of gas flow rate or the nature of the gas on mass transfer was very small in the trickle regime

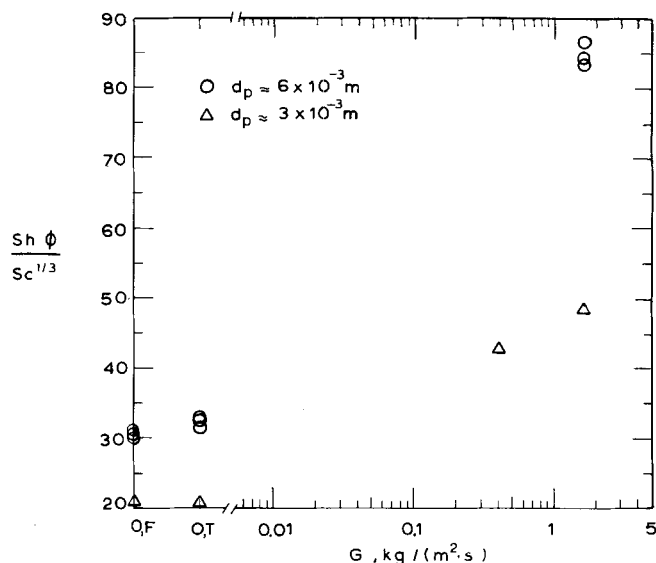


Fig. 6. Effect of gas flow rate on $Sh\phi/Sc^{1/3}$, $L = 25 \text{ kg}/(\text{m}^2 \cdot \text{s})$ and $d_p = 6 \times 10^{-3} \text{ m}$ or $3 \times 10^{-3} \text{ m}$. Pulsing with foaming at $G = 0.4$ and $d_p = 3 \times 10^{-3} \text{ m}$.

but was marked in the pulse regime, with mass transfer continuing to increase with an increase in gas flow rate at fixed liquid flow rate. These trends are in agreement with those found by other researchers, except those reported by Specchia et al. (1976). At an intermediate liquid flow rate, they reported a considerable increase in mass transfer as gas flow was increased at relatively low gas flow rates. As gas flow rate was further increased, mass transfer reached an asymptotic value or decreased slightly. These marked increases in mass transfer with gas flow rate were reported at a liquid flow rate as low as $1.6 \text{ kg}/(\text{m}^2 \cdot \text{s})$. The reasons for this difference are not clear but may be associated with the fact that their column had no inert packing in the exit section, so their flow pattern may have been different at a specified set of flow rates. We noted that at a fixed liquid rate, as gas flow was increased, pulsing began at the bottom of the column and then moved up the column. Sato et al. (1973) similarly noted such progression as liquid flow rate was increased. It would be interesting to investigate whether the lengths of the inert entrance and exit sections and the type of support screen (for example, mesh size and void fraction) influence liquid-solid mass transfer in trickle-bed systems, over a range of gas flow rates such as 0 to $1.6 \text{ kg}/(\text{m}^2 \cdot \text{s})$, both before and after the pulse regime has established itself along the whole length of the column.

CORRELATION OF RESULTS

Of previous experimental studies on mass transfer, as listed in Table 1, several are not readily comparable with our results in a brief way. Goto et al. (1975) studied crushed pellets of β -naphthol or naphthalene at Reynolds numbers up to 14 and at zero or very low gas flow rates. In the region of the same Reynolds number, their mass transfer rates were substantially higher than ours or those reported by Specchia et al. (1976). This most probably is because in the Goto et al. calculations, particles were taken to be spheres, the diameter of which was calculated as the average mesh size opening, so the true area would be considerably greater, but to an unknown degree. They studied granules, in contrast to tablets, and of a different solute, and possibly these may have been more completely wetted.

Sato et al. (1972) correlated their data in terms of an enhancement factor which was expressed as a func-

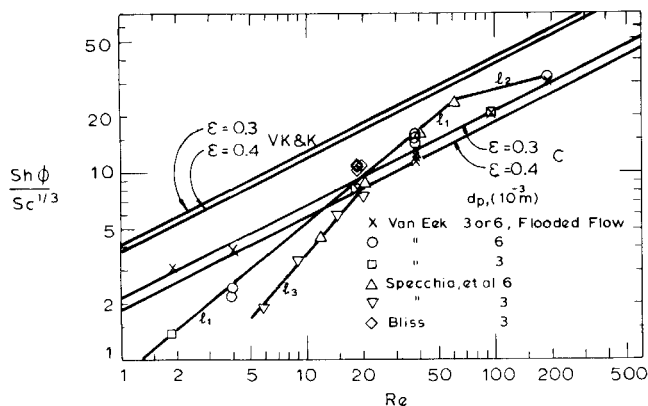


Fig. 7. Mass transfer at zero gas flow rate.

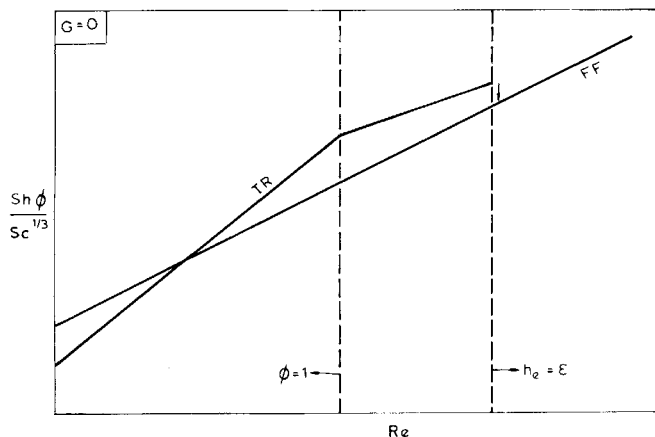


Fig. 8. Postulated effect of Re on $Sh\phi/Sc^{1/3}$ at zero gas flow rate. Log-log coordinates.

tion of a Lockhart-Martinelli parameter. These data of Sato et al. are discussed with a more detailed explanation by Hirose et al. (1976) who also introduce additional information. The Sylvester-Pitayagulsarn results (1975) as later corrected (1976) are fairly consistent with ours at $L = 5 \text{ kg}/(\text{m}^2 \cdot \text{s})$, but at $L = 25 \text{ kg}/(\text{m}^2 \cdot \text{s})$, their equation predicts values considerably lower than those measured by us. They report that k_s became independent of the liquid rate at values of L greater than $8.6 \text{ kg}/(\text{m}^2 \cdot \text{s})$, an effect which was not found by Lemay et al. (1975), Sato et al. (1972), or Hirose et al. (1976). These and other previous studies are discussed and analyzed in detail by van Eek (1977).

Mass Transfer in Absence of Gas Flow

Comparison of measured values of $k_s\phi$ at zero gas flow for the two tablet sizes with an approximate value from a stagnant film model provides orientation. This may be roughly estimated by assuming $\phi = 1$ and arbitrarily assuming that one half of the voids between the packing is filled with liquid and that the effective path length is one half of the average film thickness Δ . This gives $k_s = D/(\Delta/2) = 2D/(h_e/a_p) = 4Da_p/\epsilon$, where a_p is the outside area of the packing per unit bed volume. Measured values were about 40% of those thus estimated at $L = 0.5 \text{ kg}/(\text{m}^2 \cdot \text{s})$ but were greater than those estimated by a factor of 1.5 to 2.9 at $L = 4.8$ and by a factor of 3.5 to 6.0 at $L = 25$. At the lowest value of L , wetting is presumably not complete.

Figure 7 shows the present mass transfer results at zero gas flow rate together with those of Specchia et al. (1976) for pure water at zero gas flow rate. All data points were taken in the trickle regime except those marked X, which represent flooded flow. The raw data of Bliss (1976) were recalculated, and the values of

$Sh\phi/Sc^{1/3}$ given here are slightly different than those in his thesis. The line marked C represents the equation by Carberry (1960) for flooded flow and void fractions of 0.3 to 0.4. VK&K represents the equation by van Krevelen and Kerkels (1948) for what they call "film-like" flow, also for void fractions of 0.3 or 0.4.

In order to interpret Figure 7, certain features of it are discussed with the aid of Figure 8, which is on the same coordinates. The simplest type of correlation that could be expected for liquid-solid mass transfer in the trickle regime at zero gas flow rate would be one of the type

$$Sh\phi/Sc^{1/3} = \alpha Re^\beta \quad (2)$$

where α and β are constants.

The line marked TR represents such a correlation for the trickle regime. The line marked FF, which is the correlation for flooded flow, is of the same form as Equation (2) but with different values of α and β . In keeping with the experimental results, the two lines are shown to cross since higher values of $Sh\phi/Sc^{1/3}$ were found in flooded flow than in trickle flow at low superficial flow rates. The slope of the line FF is about 0.5 as has been reported in the literature by, for instance, Carberry (1960). The slope of the line TR is greater than 0.5, reflecting an increase in both the trickle flow Sherwood number and the wetting factor ϕ as Re increases. At some value of Re , however, the fraction of the packing wetted with flowing liquid becomes unity and no longer increases. At this point, indicated on Figure 8 by the vertical dashed line marked $\phi = 1$, the slope of the line TR changes. Now only Sh increases with Re , and the situation is one of film flow over a completely wetted packing. The slope changes to a value which is lower than 0.5, in agreement with the results reported by Hirose et al. (1974) for film flow on single spheres at higher liquid flow rates.

As Re increases, the liquid film thickness increases until, probably rather abruptly, films on adjacent particles coalesce and the bed becomes naturally flooded. At this point, indicated in Figure 8 by the vertical dashed line marked $h_e = \epsilon$, mass transfer behavior reverts to that observed in flooded flow, and at higher values of Re the applicable correlation is the line FF. Consequently, there is a step change at $h_e = \epsilon$, indicated by the arrow pointing downwards. The position of the line $h_e = \epsilon$ will depend on such variables as the particle diameter and the void fraction.

This postulated behavior explains the individual features of Figure 7. The data obtained here for 3 and 6 mm cylinders in flooded flow agreed very well with Carberry's equation

$$Sh/Sc^{1/3} = 1.15\epsilon^{-1/2}Re^{1/2} \quad (3)$$

In the trickle regime at conditions of incomplete wetting, the present results at $Re \leq 60$ including those by Specchia et al. (1976) at their higher Reynolds numbers all lie along the line l_1 . This is represented by Equation (4) with average absolute percentage deviation of 10.8%:

$$Sh\phi/Sc^{1/3} = 0.815 Re^{0.822} \quad (4)$$

The two trickle regime points at $Re = 97$ and at 190 are less than would be predicted by Equation (4). The latter point is for 6 mm cylinders, and operation is in the region in Figure 8 between the two dashed vertical lines. Wetting is complete, but the bed is not yet naturally flooded. For the former point, which is for the 3 mm cylinders, operation is probably in the region to the right of the line $h_e = \epsilon$ in Figure 8.

The equation proposed by Specchia et al. (1976) for correlation of all their data in the trickle regime at zero

gas flow rate and those of Goto and Smith (1975a) has $Sh\phi$ proportional to $Re^{0.734}$ in their nomenclature. This equation gives numerical values which agree with those from Equation (4) within about $\pm 13\%$ over the range of Reynolds numbers they studied. At $Re < 20$, their data in Figure 7 fall below what is predicted by Equation (4). It is possible that at these lower liquid flow rates their system had not reached a state of equilibrium wetting when they took their data, or that a different initial state of their bed may have led to a different level of equilibrium wetting. Several observers have noted that a long time may be required for an initially dry bed to reach equilibrium wetting and that prewetting or preflooding considerably improves the subsequent degree of wetting.

The mathematical expression for the data of Specchia et al. in Figure 7 at $Re \leq 20$ (line l_3 in Figure 7) was found by a least-squares fit to be given by Equation (5), with an average absolute percentage deviation of 4.7%:

$$Sh\phi/Sc^{1/3} = 0.266 Re^{1.147} \quad (5)$$

The point of branching from line l_1 to l_2 (the latter representing the trickle regime at zero gas flow with complete wetting) likely depends on the values of σ and σ_c [see discussion after Equation (7)], and the value of Re at which this branching takes place and $\phi = 1$ is possibly not independent of particle size. The two points available for the system benzoic acid/water and the 6 mm cylinders give the following equation for line l_2 , but additional data are needed to develop a more correct expression for this region:

$$Sh/Sc^{1/3} = 8.14 Re^{0.26} \quad (6)$$

The power on Re in Equation (6) is consistent with some findings by Miyashita et al. (1975). According to an abstract of their work, they found experimentally that for laminar flow of a liquid film on a horizontal cylinder (presumably completely wetted), the exponent of the Reynolds number was 1/9 (which agreed with their theoretical model) in their smaller Reynolds number region and increased with the Reynolds number, approaching 1/3.

The lines marked VK&K in Figure 7 represent a rearranged version of the "filmlike flow" findings of van Krevelen and Krekels (1948) who studied granular particles at liquid flow rates below $3.7 \text{ kg}/(\text{m}^2 \cdot \text{s})$ in liquid continuous or filmlike flow. In the latter case, apparently no forced flow of gas was applied (Krekels, 1972), so it would seem that this was trickle flow at zero gas flow rate. These lines [given by Equation (7)] lie well above all the data points shown in Figure 7:

$$Sh\phi/Sc^{1/3} = 4.879(1 - \epsilon)^{1/2} Re^{1/2} \quad (7)$$

Further correlations of the data represented by Equation (4) and of data of Specchia et al. (1976) taken at a different value of liquid surface tension were made by van Eek (1977). These included the effect of gravity, taken into account by the Galilei number Ga . At low liquid flow rates, the effect of liquid surface tension should be important when wetting is incomplete, and this was taken into account by the Suratman number Su and the group σ/σ_c , where σ_c is the critical surface tension of the liquid for a particular packing material as defined by Onda et al. (1967). The resulting expressions are probably a better representation of the physical situation, but they contain a greater number of terms, and there is inadequate evidence as yet of their degree of applicability.

The effect of gas flow rate is illustrated by Figures 3 through 6. For the trickle regime, where the gas flow

is nonzero but the ripple or pulse regime was not encountered, gas flow rate has little effect on mass transfer. As a general observation, its enhancing effect, if any, amounts to an increase in the mass transfer coefficient of about 10% or less.

PULSE REGIME

In turbulent flow, the rate of mass transfer may be usefully related to the degree of energy dissipation, and this approach has been used by Calderbank and Moo-Young (1961) for a number of systems including mass transfer to a single fluid in packed beds. They derived the proportionality

$$\frac{k_s d_p}{D} \propto \left(\frac{\mu}{\rho D} \right)^x \left[\frac{\rho^2 (Po/v) d_p^4}{\mu^3} \right]^y \quad (8)$$

where x and y are constants.

They then assumed that k_s was explicitly independent of d_p . After further assuming that k_s is proportional to $D^{2/3}$, $x = 1/3$ and $y = 1/4$. Heat and mass transfer coefficients, as reported by a variety of workers, were thus correlated by Calderbank and Moo-Young by Equation (9):

$$k_s Sc^{2/3} = 0.13 \left(\frac{(Po/v)\mu}{\rho^2} \right)^{1/4} \quad (9)$$

This last equation was found to hold over seven orders of magnitude of the power dissipation function $[(Po/v)\mu/\rho^2]^{1/4}/Sc^{2/3}$ for heat and mass transfer to suspended particles in turbulent fluids and to apply as well for heat and mass transfer to a single fluid in packed beds and in pipes for turbulent flow.

With two-phase flow in packed beds, various formulations of a power dissipation function are readily conceivable, and it is not clear a priori which might be preferable. Lemay et al. (1975) studied mass transfer to 6.25 mm spheres in the pulse regime at values of L between 13 and 40 $\text{kg}/(\text{m}^2 \cdot \text{s})$. They correlated their data by an equation of the Calderbank Moo-Young form utilizing the power dissipation by the liquid phase expressed per unit mass of external liquid holdup, designated as E_L' , which resulted in Equation (10):

$$k_s Sc^{2/3} = 0.20 (E_L' \mu_L / \rho_L)^{1/4} \quad (10)$$

If the Calderbank, Moo-Young assumption that k_s is proportional to $D^{2/3}$ is retained but k_s is taken to be a function of d_p , it can be shown that in the context of the present study Equation (8) can be formulated as

$$\frac{k_s d_p'}{D} = m \left[\frac{E_L' (d_p')^4 \rho_L^3}{\mu_L^3} \right]^n \left(\frac{\mu_L}{\rho_L D} \right)^{1/3} \quad (11a)$$

or

$$Sh/Sc^{1/3} = m K_o^n \quad (11b)$$

where m and n are constants and the bracketed expression on the right-hand side is the Kolmogoroff number.

The data obtained in the pulse regime in the present study are plotted utilizing each of these two approaches in Figures 9 and 10. The results of Bliss are slightly higher than those of van Eek for reasons that are not completely clear. Start-up was the same, but in the Bliss procedure, after measurements were made with flooded flow, the bed was drained relatively quickly which may have given a slightly higher wetted fraction and/or perhaps a lower liquid holdup and higher superficial velocity.

Figure 9 shows $k_s \phi Sc^{2/3}$ as a function of $E_L' \mu_L / \rho_L$. In evaluating E_L' , the experimentally measured values of $(-\Delta P/z)_{LG}$ were used, and h_e was calculated from the findings of Sato et al. (1973a). The line marked

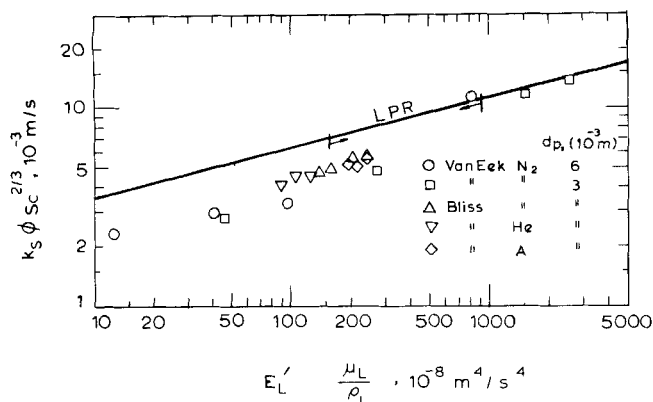


Fig. 9. Effect of E_L' (μ_L/ρ_L) on $k_s \phi Sc^{2/3}$. Pulse regime.

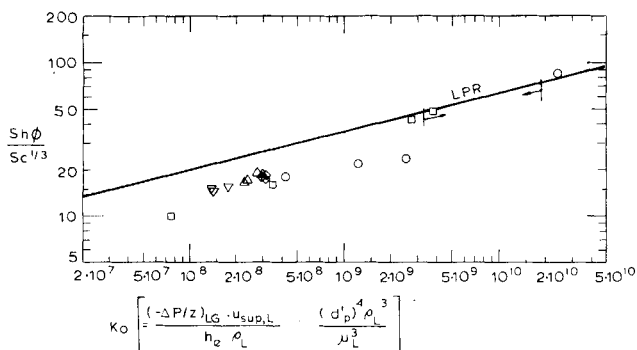


Fig. 10. Effect of Ko on $Sh \phi / Sc^{1/3}$. Pulse regime. See Figure 9 for legend.

LPR represents the correlation of Lemay et al. (1975), Equation (10). These researchers studied experimental conditions for which E_L' varied between 1.75 and 10 W/kg (1 W/kg = 1 m²/s³), and $E_L'(\mu_L/\rho_L)$ varied between 160×10^{-8} and 906×10^{-8} m⁴/s⁴. This is indicated on Figure 9 as the region between the bases of the two arrows. The sections of the line LPR outside the two arrows are extrapolations.

The present results at $L = 25$ kg/(m²·s) for 3 and 6 mm cylinders (represented by the top three points) agree well with the findings of Lemay et al., the average deviation from their equation being 6.3%. All the other results, which were at a liquid flow rate of 5 kg/(m²·s), but still in the pulse regime, fall below the Lemay et al. correlation by an average of about 35%. A least-squares fit of these lower data points retaining the exponent of one fourth resulted in a proportionality constant of 0.13 instead of 0.20 in Equation (10). This is identical to the Calderbank, Moo-Young equation, Equation (9). The average absolute percent deviation was 8.5%. It will be necessary to conduct further experiments at liquid flow rates above 5 kg/(m²·s) and especially between 5 and 13 kg/(m²·s) to truly understand why mass transfer in the pulse regime follows a different behavior at high liquid flow rates than at the intermediate liquid flow rate of 5 kg/(m²·s), with the proportionality constant changing to 0.20 from 0.13. Other than L , the heights of the inert entrance and exit sections may be important and may have a different effect at intermediate values of L than at high values of L .

Figure 10 shows the present data plotted as $Sh \phi / Sc^{1/3}$ vs. Ko , in accordance with Equation (11b). The line marked LPR in Figure 10 again represents the equation by Lemay et al. which, in terms of the coordinates used in this figure, is given by

$$Sh \phi / Sc^{1/3} = 0.20 Ko^{0.25} \quad (12)$$

For the conditions studied by Lemay et al., Ko varied between 33×10^8 and 188×10^8 , the range between the bases of the two arrows in Figure 10. Here, Ko varied between 0.76×10^8 and 240×10^8 .

Again, present results at $L = 5$ kg/(m²·s) fall below the Lemay et al. correlation by an average of 34%. A least-squares fit of all the lower data points in Figure 10 was performed to an equation of the type (11b) and is shown as Equation (13):

$$Sh \phi / Sc^{1/3} = 0.334 Ko^{0.202} \quad (13)$$

The average absolute percent deviation of the data from this equation is 7.2%.

If the Calderbank, Moo-Young assumption that k_s is explicitly independent of d_p is valid, then Ko should appear to the 0.25 power in Equation (13). It would appear that this assumption is not quite true, but additional study is needed in the intermediate liquid-flow rate area of the pulse regime to fully substantiate Equation (13). It is perhaps surprising that the Kolmogoroff approach works this well here, since it is unclear from theory whether or not the level of turbulence is adequate for this approach to be made.

Power dissipation here is always much greater in the gas phase than in the liquid phase, which suggests that E' should be reformulated to contain ($u_{sup,G} + u_{sup,L}$) instead of $u_{sup,L}$, which leads to different numerical values of Ko . However, use of Ko_{G+L} did not correlate the data as well as Ko_L , and it appeared that this approach overemphasized the effect of the gas velocity.

In a few of the pulsing runs, foaming occurred, but foaming did not seem to affect significantly the dependence of k_s on E_L' . However, the dependence of E_L' on liquid and gas flow rates is probably different in foaming pulsing flow than in the ordinary pulse regime.

Effect of Gas Density

Most trickle-bed reactors are used for hydrogenation, and in the petroleum industry, they are usually operated under pressure. The gas phase may contain considerable quantities of components other than hydrogen. On the other hand, laboratory studies usually have been made at 1 atm pressure, utilizing air or nitrogen. There is little information to indicate the effect of gas density on the liquid-solid mass transfer coefficient. The studies here (Bliss, 1976) utilizing helium, nitrogen, and argon show the effect of a tenfold variation in gas density under a limited set of circumstances, the dissolution of 3 mm cylinders at the fixed liquid flow rate of 5 kg/(m²·s). A variety of methods of correlation were attempted, but neither gas velocity, gas phase Reynolds number, nor gas mass flux was capable of correlating the mass transfer coefficients for all three gases employed. From Figures 9 and 10, it is noteworthy that the mass transfer coefficient does not depend explicitly upon gas density if it is correlated in terms of an energy dissipation function.

Further Studies

Some of the variables which still cause considerable uncertainty in predicting mass transfer in this type of contactor are:

1. The nature of the flow pattern, for example, natural flooding in contrast to trickle flow, encountered with relatively small packing.
2. The length of the time required for a system to come to steady state, especially at low liquid flow rates.
3. The change in hydrodynamic flow pattern with axial distance. Trickle flow may occur at the top and pulsing flow at the bottom. The nature of this pattern and hence measurements reported from laboratory studies may be significantly affected by the height of the dissolving section and by the heights and design of en-

trance and exit sections.

4. The degree of wetting. This is affected by interfacial tension and other variables. Measurements of mass transfer are needed in systems with different wetting characteristics than that of water with benzoic acid or other closely related slightly soluble organic solids.

ACKNOWLEDGMENT

The gas-liquid distributor was designed and fabricated by the Department of Mining Engineering, Technische Hogeschool Delft, The Netherlands. Benzoic acid was pelletized by Merck & Company, Inc., Rahway, New Jersey, under the supervision of Dr. George Wildman. Inert packing was supplied by the Norton Company and Chemetron Corporation. Helpful comments from Dr. Tsutomu Hirose are appreciated. An early portion of the study was financially supported by the National Science Foundation.

NOTATION

- A_c = cross section of the column, m^2
 A_p = total external area of the packing in the dissolving section, m^2
 c = concentration of solute in the bulk of the liquid, kg/m^3 ; c_{exit} for liquid leaving the column, c_{sat} for saturation concentration
 D = diffusivity of solute in the liquid, m^2/s
 d_p = true particle diameter, m
 d_p' = equivalent particle diameter of a sphere having the same surface area as the particle in question, m ; $d_p' = [A_p/(n_p \cdot \pi)]^{1/2}$
 E_L = power dissipation by the liquid phase per unit volume of bed, W/m^3 , $= (-\Delta P/z)_{LG} \cdot u_{sup,L}$
 E_L' = power dissipation by the liquid phase per unit mass of external liquid holdup, $= E_L/(h_e \rho_L)$, $W/kg = 1 m^2/s^3$
 G = superficial gas mass flow rate, $kg/(m^2 \cdot s)$
 Ga = liquid phase Galilei number $= g(d_p')^3 \rho^2/\mu^2$
 g = gravitational acceleration, m/s^2
 h_e = external liquid holdup, m^3 of liquid/ m^3 of bed volume
 Ko = liquid phase Kolmogoroff number $= E_L'(d_p')^4 \rho_L^3/\mu_L^3$
 k_s = liquid-solid mass transfer coefficient, m/s
 L = superficial liquid mass flow rate, $kg/(m^2 \cdot s)$
 L_v = superficial volumetric liquid flow rate, $m^3/(m^2 \cdot s)$
 n_p = number of particles in the dissolving section
 $(-\Delta P/z)_{LG}$ = two-phase pressure drop per unit length of column, for gas-liquid flow, N/m^3
 Po/v = power dissipated per unit volume of continuous phase, W/m^3
 Re = liquid phase Reynolds number, $= u_{sup} \rho d_p'/\mu$ (same as Ld_p'/μ)
 Sc = Schmidt number of liquid, $= \mu/(\rho D)$
 Sh = Sherwood number of liquid, $= k_s d_p'/D$
 Su = liquid phase Suratman number, $= \sigma d_p' \rho/\mu^2$
 $u_{sup}, u_{sup,L}$ = superficial liquid velocity in the column, m/s
 $u_{sup,G}$ = superficial gas velocity in the column, $= G/\rho_G$, where ρ_G is evaluated at the local column conditions of pressure and temperature (m/s)

Greek Letters

- Δ = average film thickness, m
 ϵ = void fraction in packed bed
 μ, μ_L = viscosity of the liquid phase, $kg/(m \cdot s)$
 μ_G = viscosity of the gas phase, $kg/(m \cdot s)$
 ρ, ρ_L = density of the liquid phase, kg/m^3
 ρ_G = density of the gas phase, kg/m^3
 σ = surface tension of the liquid phase, N/m
 ϕ = fraction of the external surface area of the packing (in the dissolving section) that is wetted

with flowing liquid; ϕ varies between zero and one

LITERATURE CITED

- Bliss, G. S., "Effects of the Gas Phase on Liquid-Solid Mass Transfer in a Trickle Bed," S.M. thesis, Mass. Inst. Technol., Cambridge (1976).
 Calderbank, P. H., and M. B. Moo-Young, "The Continuous Phase Heat and Mass Transfer Properties of Dispersions," *Chem. Eng. Sci.*, **16**, 39 (1961).
 Carberry, J. J., "A Boundary-Layer Model of Fluid-Particle Mass Transfer in Fixed Beds," *AIChE J.*, **6**, 460 (1960).
 Charpentier, J.-C., M. Bakos, and P. Le Goff, "Hydrodynamics of Two-Phase Concurrent Downflow in Packed Bed Reactors," paper presented at the 2nd Congr. on "Quelques applications de la Chimie Physique," Veszprem, Hungary (1971).
 Gianetto, A., Personal communications, Istituto di Chimica Industriale del Politecnico di Torino, Torino, Italy (Sept. and Dec., 1976).
 Goto, S., J. Levec, and J. M. Smith, "Mass Transfer in Packed Beds with Two-Phase Flow," *Ind. Eng. Chem. Process Design Develop.*, **14**, 473 (1975).
 Goto, S., and J. M. Smith, "Trickle-Bed Reactor Performance: Part I. Holdup and Mass Transfer Effects," *AIChE J.*, **21**, 706 (1975a).
 Hirose, T., Y. Mori, and Y. Sato, "Solid-Liquid Mass Transfer in Falling Liquid Films on Single Spheres," *J. Chem. Eng. Japan*, **7**, 19 (1974).
 ———, "Liquid-to-Particle Mass Transfer in Fixed Bed Reactor with Cocurrent Gas-Liquid Downflow," *ibid.*, **9**, 220 (1976).
 Krekels, J. T. C., Personal communication, Dutch State Mines, Geleen, The Netherlands (Sept., 1972).
 Lemay, Y., G. Pineault, and J. A. Ruether, "Particle-Liquid Mass Transfer in a Three-Phase Fixed Bed Reactor with Cocurrent Flow in the Pulsing Regime," *Ind. Eng. Chem. Process Design Develop.*, **14**, 280 (1975).
 Miyashita, H., K. Saeki, H. Ueda, and T. Mizushima, "Transport Phenomena in Laminar Flow of a Liquid Film on a Horizontal Cylinder," *Kagaku Kogaku Ronbunshu*, **1**, 610 (1975); abstract in *J. Chem. Eng. Japan*, **8**, 511 (1975).
 Onda, K., H. Takeuchi, and Y. Koyama, "Effect of Packing Materials on the Wetted Surface Area," (in Japanese), *Kagaku Kogaku*, **31**, 126 (1967).
 Sato, Y., T. Hirose, F. Takahashi, and M. Toda, "Performance of Fixed-Bed Catalytic Reactor with Co-current Gas-Liquid Flow," *Pacific Chem. Eng. Congress*, Session 8, Paper 8-3, p. 187 (1972).
 ———, "Pressure Loss and Liquid Holdup in Packed Bed Reactor with Cocurrent Gas-Liquid Down Flow," *J. Chem. Eng. Japan*, **6**, 147 (1973a).
 ———, and Y. Hashiguchi, "Flow Pattern and Pulsation Properties of Cocurrent Gas-Liquid Downflow in Packed Beds," *ibid.*, **6**, 315 (1973).
 Satterfield, C. N., "Trickle-Bed Reactors," *AIChE J.*, **21**, 209 (1975).
 Specchia, V., G. Baldi, and A. Gianetto, "Solid-Liquid Mass Transfer in Trickle Bed Reactors," *Proceedings of the Fourth International/Sixth European Symposium on Chemical Reaction Engineering*, Heidelberg, West Germany (April 1976), p. 390, DECHEMA, Frankfurt am Main (1976).
 Sylvester, N. D., and P. Pitayagulsarn, "Mass Transfer for Two-Phase Cocurrent Downflow in a Packed Bed," *Ind. Eng. Chem. Process Design Develop.*, **14**, 421 (1975); correction, *ibid.*, **15**, 360 (1976).
 van Eek, M. W., "Liquid-Solid Mass Transfer in Packed Beds in the Presence of a Downward Cocurrent Gas-Liquid Flow," Ph.D. thesis, Mass. Inst. Technol., Cambridge (1977).
 van Krevelen, D. W., and J. T. C. Krekels, "Rate of Dissolution of Solid Substances. Part I. Rate of Mass Transfer in Granular Beds (Physical Dissolution)," *Recueil Des Travaux Chimiques Des Pays-Bas*, **67**, 512 (1948).
 Weekman, V. W., Jr., and J. E. Myers, "Fluid-Flow Characteristics of Concurrent Gas-Liquid Flow in Packed Beds," *AIChE J.*, **10**, 951 (1964).

Manuscript received July 22, 1977; revision received January 30, and accepted March 27, 1978.